



Venezia2021

Programma di ricerca scientifica per una laguna “regolata”

Linea 2.2

*Inquinanti prioritari e rilascio di sostanze
pericolose dal sedimento*

D2.2.4.3

*Rapporto tecnico-scientifico sulle
misure SOD*

**Simone Leoni, Janusz Dominik,
Daniele Cassin, Giorgia Manfè,
Davide Tagliapietra, Francesco Acri and
Roberto Zonta (CNR-ISMAR)**

12/04/2022

Summary

RIASSUNTO	3
ABSTRACT	3
1. INTRODUCTION	4
2. MATERIAL AND METHODS	6
2.1 Study area	6
2.2 Sediment characteristics	7
2.3 Characteristics of the benthic chambers	8
2.4 Preparation and use of the chamber in situ	9
2.5 Blank correction	10
2.6 SOD rate calculation	10
2.7 Replicates	11
3. RESULTS AND DISCUSSION	13
3.1 Sediment characteristics	13
3.2 SOD rate distribution with site and time	14
3.3 Operation of the MOSE - Estimating DO depletion due to SOD during the closing periods.	18
4. CONCLUSIONS	22
Acknowledgements	22
Funding	23
Author Contributions	23
References	24

RIASSUNTO

Il sistema MOSE è entrato in funzione alle tre bocche di porto dal mese di ottobre 2020, per la protezione di Venezia e la sua laguna da allagamenti conseguenti ad eventi di alta marea nel Mar Adriatico. Se questo aumenta la prospettiva della difesa fisica, in che modo il nuovo stato di laguna “regolata” influirà sul funzionamento del sistema? In particolare, il bilancio dell’ossigeno disciolto nella colonna d’acqua può essere impoverito dall’aumento dei tempi di ricambio idrico, che avvengono con i flussi di marea. Il sedimento è uno dei principali fattori di consumo di ossigeno nella colonna d’acqua; per questo motivo la sua domanda di ossigeno (SOD) è stata studiata per la prima volta, in situ, in quattro aree lagunari durante il 2021. Il tasso SOD, misurato con camere bentiche costruite in casa, è risultato variare nelle diverse aree e con le stagioni, con valori più elevati nei siti più confinati e significativamente più bassi in quelli appartenenti alla laguna aperta. Unicamente sulla base dei valori di SOD ottenuti, sono stati stimati i tempi di consumo di ossigeno disciolto nella colonna d’acqua alla chiusura del MOSE, a partire dai valori di saturazione fino al limite dell’ipossia. Il tempo stimato – nell’intervallo di temperatura tra 11.73 e 33.27 °C – ha mostrato che nei siti più confinati il sedimento può determinare un’importante azione di consumo dell’ossigeno disciolto, anche in situazioni di temperature non particolarmente elevate per la laguna.

ABSTRACT

From October 2020, the MOSE system went into operation in the three seaward inlets to protect Venice and its lagoon from flooding due to high tide events in the Adriatic Sea. While this increases the prospect of the physical defense, how will the new status of “regulated” lagoon affect the functioning of the system? In particular, the dissolved oxygen balance in the water column can be affected by the increase in water renewal times with the tide. Sediment is one of the main factors of oxygen consumption in the water column, and for this reason its oxygen demand (SOD) has been studied for the first time, in situ, throughout the 2021 in four lagoon areas. SOD rate, measured with home built benthic chambers, was found to vary in the different areas and with the seasons, with higher values in the more confined sites, and significantly lower in those belonging to the open lagoon. On the basis of the obtained SOD rate values alone, the consumption times of dissolved oxygen in the water column from saturation values to hypoxia were estimated at the closing of the MOSE. Estimated time – in the range 11.73 to 33.27 °C – showed that in the more confined sites the sediment can determine an important depleting action on dissolved oxygen, even in situations of temperatures not particularly high for the lagoon.

Keywords: benthic chambers, climate changes, lagoons, MOSE system, oxygen depletion, sediment oxygen demand (SOD), Venice.



1. INTRODUCTION

Dissolved oxygen in the water column (DO) is essential for aquatic life and its concentration is a direct indicator to evaluate the ecosystem health (Vellidis et al., 2006; Macpherson et al., 2007). Low DO concentrations are harmful to the aquatic life, to the point that hypoxia ($< 2.8 \text{ mg L}^{-1}$) or anoxia (absence of oxygen) events entail damages to the population structure, and ecosystem function (Diaz and Rosenberg, 1995, Altieri and Diaz, 2019).

Oxygen solubility in water is inversely proportional to temperature, so it decreases in warmer waters (Garcia and Gordon, 1992). The threat from climate changes is increasing and one of the main consequences is the decrease in oxygen due to global warming, in different aquatic environments (Breitburg et al., 2018, Pitcher et al., 2021).

Other processes decreasing DO concentration include water column stratification, reducing the downward supply of O_2 -rich surface waters (Manabe et al., 1991; Collins et al., 2013; Breitburg et al., 2018), land use and agricultural activities that implicate nutrient enrichment in water (Kemp et al., 2005), and nocturnal oxygen consumption via plant respiration (Caraco and Caraco, 2002).

Major sources of DO in the sediment-water column are photosynthetic production and re-aeration from the atmosphere, whereas natural sinks are sediment oxygen demand (SOD) and biochemical oxygen demand (BOD) of the water column (Rounds and Doyle 1997; Rong et al., 2016).

SOD is the rate at which DO is removed from the water by biochemical processes in the sediment (Hatcher, 1986). It includes depletion due to both biological respiration of benthic organisms (biological SOD, BSOD) and chemical oxidation of reduced compounds (chemical SOD, CSOD) arising from anaerobic metabolism (Walker and Snodgrass, 1986; Chau, 2002; Doyle and Lynch, 2005).

BSOD is governed by aerobic heterotrophs that utilize organic material as an energy source (Middelburg et al., 2005); CSOD involves anaerobic bacteria which degrade organic matter releasing reduced compounds (mainly of nitrogen, manganese, iron) that react with molecular oxygen (Rounds & Doyle, 1997; Todd et al., 2010).

In surface waters, oxygen concentrations are strongly dependent on air-sea exchange, whereas in bottom waters, especially in shallow systems such as lagoons, exchange across the sediment-water interface is often significant (Pitcher et al., 2021). Due to the high sediment surface area to water volume ratios, lagoon sediments influence the dynamics of oxygen and play an important regulatory function for the whole ecosystem (Giordani et al., 2008, Brigolin et al., 2021).

Lagoons are also place with high organic matter inputs (Viaroli et al., 2008). Settled organic material is actively decomposed by microbial processes and the DO level consequently decreases (Castel et al., 1996). Systems with longer water residence times and stratified water columns are more prone to be subjected to hypoxia events (NRC, 2000).

Serious anoxic events diffusely occurred in the Venice Lagoon (Fig. 1) in the hot months of the 1980s (Sfriso et al., 1987, Sfriso et al., 1995, Zirino et al., 2016), due to the rot of *Ulva rigida* after impressive blooms. Since 1990, a progressive improvement of the situation has taken place (Sfriso and Marcomini, 1996) thanks to a concomitance of climatic situations, increased water turbidity and biomass harvesting.

While events of this severity did not recur after the 1980s, hypoxia/anoxia events have been observed in some sectors of the lagoon since the early 2010s (Bernardi Aubry et al., 2020), although generally lasting less than 24 hours (ISPRA and ARPAV, 2016; 2018; 2021).

A new era of “regulated flows” with the Adriatic Sea began for the lagoon in October 2020, when the MOSE system was operated for the first time (Mel et al., 2021) to defend Venice and the lagoon against flooding during high sea-level events. The MOSE system (Scotti, 2005; Trincardi et al., 2016) consists of mobile gates clustered into barriers installed on the bottom of the three seaward inlets of the lagoon, which rise up and temporarily seal off the waterbody from the sea during high tide events.

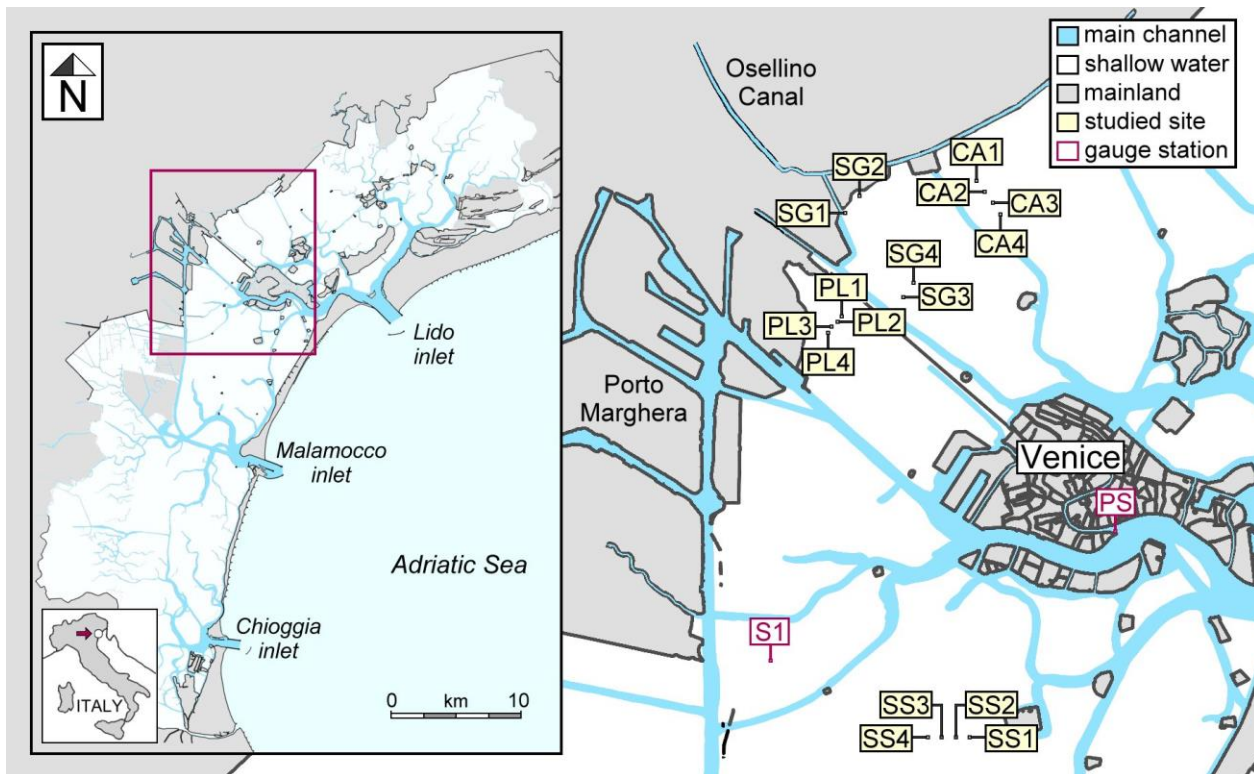


Figure 1. Location of the 16 measurement sites in the four selected areas of the Venice Lagoon (in the insert). SP (45°24.7934 N 12°16.4518) and PS (45°25.8656 N 12°20.1826 E) identify the DO gauge station of the SAMANET network and the tide gauge of Punta Salute (managed by the Venice Municipality), respectively.

Although the MOSE system can potentially be operated in the future to improve the water exchange with the sea through appropriate maneuvers with the barriers, it is expected to increase the water renewal time in the lagoon as a whole (Ferrarin et al., 2013). Due to the sea level rise and the higher incidence of severe storms, an increase in the periods of entry into operation of the MOSE is expected in the future, to prevent flood events in the lagoon (Lionello, 2012; Cavaleri et al., 2020).

Moreover, it is worth observing how an increase in the frequency of summer heat waves due to climate change (Molina et al., 2020) is occurring in the Mediterranean region, which may lead to a greater duration and severity of hypoxic events in the lagoon (Brigolin et al., 2021).

In this context, it is important to investigate the role of sediments on the DO balance of lagoon waters, and how this will be affected due to prolonged closing times of the MOSE. The aim of the study was to investigate the variations in space and time of the SOD rate, which was never been determined in situ in the Venice Lagoon.

SOD rate was measured in the 2021 in four test areas (16 sites, which location is shown in Fig. 1) by means of built in house benthic chambers. The study of sediment processes that determine the rate of oxygen consumption was beyond the objectives of the study. Nevertheless, the characteristics of the sediment in the 16 measurement sites were determined for comparison with the values of the SOD rate.

A further objective of the study was the evaluation of how much the oxygen consumption of the sediment can affect the concentration of DO in the water column, during the closing events of the MOSE.

2. MATERIAL AND METHODS

2.1 Study area

Venice Lagoon is widely described elsewhere in terms of functioning and ecosystem characteristics (e.g. Zonta et al., 2018 - and references therein). With a surface area of 550 km² and a mean water depth of about 1 m, it includes islands, tidal marshes, mudflats and a complex network of tidal channels up to 10 meters deep (Fig.1). Shallow water areas account for 75% of the total surface area (ca. 415 km²). The lagoon is linked to the Adriatic Sea by three seaward inlets (Lido, Malamocco and Chioggia), which enable the exchange of water during tidal cycles. The mean tidal excursion is 30 and 80 cm in neap and spring tide conditions, respectively (Zaggia et al., 2007).

Four shallow water areas have been selected for the study (Fig. 1), named *Campalto* (CA), *San Giuliano* (SG), *Pili* (PL) and *Sacca Sessola* (SS). In each area, four sites were identified for the SOD rate measurements and numbered from 1 to 4, for a total of 16 sites.

The sites of the CA area were arranged along a perpendicular to the mainland interface at a distance of about 200 m from each other, while the sites of the PL area were arranged along a parallel line of about 210 m, facing the easternmost sector of the industrial area of Porto Marghera. In the SG area, two sites were closer to the mainland (SG1 and SG2) and the other two sites (SG3 and SG4) were located further south, towards the open lagoon north of the City of Venice; of the former, one (SG1) was located in the shallow waters of the mouth of the Osellino canal, at 47-km-long watercourse draining a crop area of 50 km² (Zonta et al., 2005). The distance of SG1 - SG2 from SG3 - SG4 was about 1400 m.

CA, SG and PL areas are located close the lagoon-mainland interface, which has higher water renewal times (Cucco and Umgiesser, 2006; Ferrarin et al., 2013), lower salinity (Guerzoni and Tagliapietra, 2006) and finer-sized sediments (Zonta et al., 2018) than the more open lagoon, to which SS area belong.

The lagoon sector which includes CA, SG and PL areas is classified as a “*marginal*” or “*restricted*” water body, based on the classification of the Water Framework Directive (WFD), as a result of the resolution of the transition gradient in discrete water bodies in the lagoon (Tagliapietra et al., 2011; ARPAV, 2018). This sector, located near the historic center of Venice, is particularly vulnerable to low oxygen situations in the summer months, (ISPRA and ARPAV, 2016; 2018; 2021).

The lagoon sector that includes the SS area is instead classified as “*open lagoon*”, characterized by greater salinity, water exchange and bathymetry than the previous one due to the proximity to the seaward inlets that allow water exchange from the Adriatic Sea. Measurement sites in the SS area were located along a perpendicular to the mainland-lagoon interface at a distance of about 200 m from each other.

The Venice Water Authority (Superintendence of Public Works, Italian Ministry of Infrastructures) manages a DO% measurement network in the lagoon (named SAMANET), including station S1 (Fig. 1) that is located not far from the study’s measurement areas. The station is subjected to a greater water exchange than most of our measurement sites, thanks to its proximity to main tidal channels. Consequently, the concentration of DO in the water column is assumed to be generally higher in station S1 than in our sites. In the warm months from June to September of the period 2018-2021 (Table 1) the 9.2 - 31.3% and 1 - 11% of the hourly values of DO recorded by the station were lower than 50 and 30%, respectively.

Measurements of the SOD rate were carried out approximately monthly in the period March - November 2021 in the 16 sites. Geographic coordinates of site and bathymetric heights are shown in Table 2, referring to the zero level of the tide in the lagoon.

Table 1. Number of cases (and percentage) of hourly DO data below 30 and 50%, recorded from June to September in the period 2018 - 2021. Data from SAMANET measuring network.

Year	DO < 30% # of cases	DO < 30% percentage	DO < %50 # of cases	DO < %50 percentage
2018	321	11.0%	916	31.3%
2019	111	3.8%	457	15.6%
2020	176	6.0%	622	21.2%
2021	28	1.0%	269	9.2%

Table 2. Coordinates in the WGS84 reference system and bathymetric height of the 16 sites; the latter refers to the zero-tide level recorded by the Punta Salute tide gauge (PS, Fig. 1).

SITE	CA1	CA2	CA3	CA4	SG1	SG2	SG3	SG4
latitud. N	45° 28.6095'	45° 28.5156'	45° 28.4461'	45° 28.3525'	45° 28.3775'	45° 28.5035'	45° 27.7413'	45° 27.8186'
longit. E	12° 18.4965'	12° 18.5723'	12° 18.6865'	12° 18.7773'	12° 17.0104'	12° 17.1360'	12° 17.5941'	12° 17.6936'
depth (m)	0.22	0.26	0.41	0.52	0.28	0.24	0.57	0.56
SITE	PL1	PL2	PL3	PL4	SS1	SS2	SS3	SS4
latitud. N	45° 27.5210'	45° 27.4875'	45° 27.4630'	45° 27.4403'	45° 24.2138'	45° 24.2252'	45° 24.2246'	45° 24.2294'
longit. E	12° 16.9414'	12° 16.9200'	12° 16.8984'	12° 16.8728'	12° 18.6400'	12° 18.4768'	12° 18.3308'	12° 18.1776'
depth (m)	0.47	0.49	0.53	0.53	0.86	0.92	1.05	1.08

2.2 Sediment characteristics

Small sediment cores (length 10 cm, diameter 6.4 cm) were collected in the 16 sites in May 2021 by means of a piston corer, taking care not to disturb the upper sediment layers. Two sediment samples were obtained from each core, corresponding to the surface (0-1) and sub-surface (1-2 cm) first layers. Samples were sieved through a 1 mm Teflon mesh to remove debris and organic fragments, and then carefully homogenized.

An aliquot of about 2 g of wet sediment was weighed and dispersed in distilled water before grain-size measurement with a laser diffraction particle size analyzer (Mastersizer 2000, Malvern Instruments, Malvern, U.K.). The instrument provided the volumetric percentage of particles belonging to 100 diameter classes in the range 0.1 to 2000 μm .

Total nitrogen (TN) and total carbon (TC) were determined on duplicate samples using a ThermoFisher Flash 2000 IRMS Elemental Analyzer (EA, ThermoFisher Scientific Inc., Aurora, OH, USA). Samples for total organic carbon (TOC) measurements were first decarbonated with HCl 1.5 N. Determined by replicate analyses of the same sample, each measurement had an average standard deviation (STD) of $\pm 0.01\%$ for TN and $\pm 0.07\%$ for TOC. Total inorganic carbon (TIC) was calculated as the difference between TC and TOC and converted to carbonates, assuming that it is entirely bound as CaCO_3 .

Water content (W_c) was determined from an aliquot of sample dried in an oven at 105 °C until it reached a constant weight (Percival and Lindsay, 1997). Based on variation coefficients of 5 replicates measurements in 3 sediment samples, the analytical error of W_c determination was less than 0.88%. W_c was not corrected for salt, as this correction is negligible.

Sediment porosity (%) was calculated following Hobbs (1983), as described in Zonta et al. (2021). Organic matter (OM) content was calculated as 1.7 TOC in %, and its density of 1.25 g cm^{-3} was assumed (Avnimelech et al., 2001). Density of mineral fraction was calculated assuming densities of CaCO_3 and of the remaining Al-Si fraction of 2.8 g cm^{-3} and 2.65 g cm^{-3} , respectively.

2.3 Characteristics of the benthic chambers

Benthic chambers are used to incubate in situ a known volume of water above a given sediment surface, measuring over time the deployment of the DO concentration in the isolated water.

The PVC cylindrical benthic chambers were made in house (Fig. 2), introducing some changes to the commonly used design for SOD measurements (Murphy and Hicks, 1986; Coenen et al., 2019). A method for measuring the SOD flow rate in situ has not been standardized (Coenen et al., 2019), and it may be worth experimenting with any technical improvements.

Chambers had an internal diameter of 30 and a height of 27 cm, 6 cm of which are intent to be driven into the sediment; the opacity of the material inhibited the photosynthesis during incubation. The lower edge of the cylinder was tapered to facilitate the insertion of the chamber into the sediment.

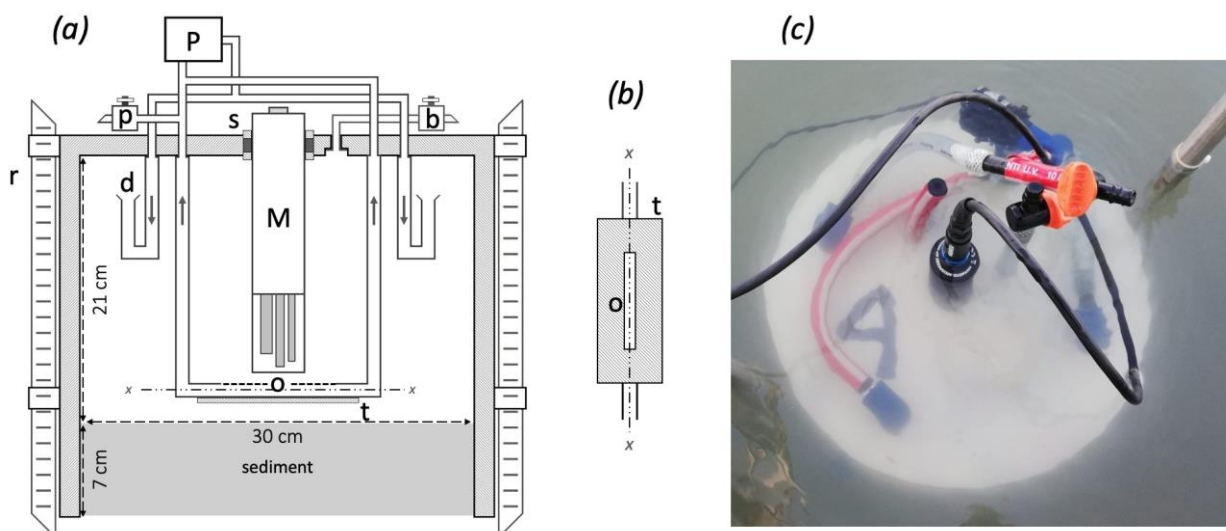


Figure 2. (a): schematic drawing of the SOD chamber (not in scale): pump (P); funnel-shaped flow diffusers (d); pump priming cock (p); air bleed cock (b); multiprobe (M); centimeter steel rods, integral with the chamber (r); composite sleeve in PVC and Plastazote® (s); rectangular suction opening (o); PVC shielding plate (t). (b): detail of the suction opening (o). (c): photo of a chamber being immersed in the water column.

Two centimeter-steel rods, made integral with the chamber, allowed the chamber to be driven into the sediment at the correct level of penetration while aboard a boat. As the two bars protruded from the base of the chamber by 15 cm, they also strengthened the stability of the apparatus once it has been driven into the sediment. A housing was present on the head of the benthic chamber to allow it to be pushed into the sediment, by means of a wooden pole, in the case of sites with sediments that have a greater sandy component.

A multiparameter water quality probe (Aquaprobe AP 2000, Aquaread Ltd, England) was inserted in the centre of the chamber to measure dissolved oxygen (optically, mg L^{-1}), temperature ($^{\circ}\text{C}$), pH, turbidity (FTU), and water depth (cm). The probe was mounted vertically in the center of the chamber, thanks to a sleeve consisting of three layers of material (Plastazote® compressed between two layers of PVC), which maintains the hermetic seal of the chamber. The probe was connected to a data-logger (Aquameter, Aquaread Ltd, England), programmed to acquire data every 5 minutes, but allowing instantaneous readings.

The chambers exposed a 0.071 m^2 area of sediment to 14.6 L enclosed water; correction was made for the volume occupied by both multiprobe and hydraulic circuits inside the chamber. Several tests were carried out to verify that the benthic chamber was completely sealed once it was embedded in the sediment.

A pump powered by a 12-volt lead-acid rechargeable battery was used for continuously recirculate the water inside the chamber. Blade shape of the pump propeller was modified to reduce its flow rate to 100 L h^{-1} ; this

means that the volume of incubated water was completely recirculated in about 9 minutes. The water circuit inside the chamber has a “recirculating fountain” configuration. The water intake (Fig. 2b), located under the probe, gently picked up the water from about 2 cm above the water-sediment interface; it consisted of a rectangular opening shielded towards the sediment by a thin sheet of PVC, to prevent the aspirated flow from causing the sediment to be resuspended. The outlet took place through two diffusers that directed the flow towards the upper part of the chamber.

The purpose of the water circulation is to achieve an approximately uniform DO concentration within the chamber, avoiding the occurrence of vertical concentration gradients and making substantially irrelevant the distance of the probe from the sediment surface.

In natural systems, a diffusive boundary layer (DBL) (Jørgensen and Revsbech, 1985; Glud et al., 1994; Glud, 2008) at the sediment water interface reduces the oxygen uptake and may lead to an underestimation of the SOD rate (Doyle and Rounds, 2003). DBL effectiveness is inversely related to the water flow velocity above the interface with the sediment. Inside the chamber, the water intake designed to suck the water near the interface with the sediment, has the purpose of counteracting the formation of DBL during the measurement or - at least - to reduce the “effective DBL thickness” (Jørgensen and Des Marais, 1990). In any case, diffusive oxygen uptake rate in coastal marine sediments makes roughly only a half of the total uptake rate, the rest being due to irrigation and fauna respiration (Glud, 2008).

In all the measurements carried out in this study with the benthic chambers, the same water recirculation speed was set, to ensure repeatability and comparability of the measurement.

On the other side, sediment resuspension within the chamber would increase the surface area of the bottom material in contact with water, leading to an overestimation of the SOD rate (Doyle and Rounds, 2003). Therefore, any effort was made in the set-up of the benthic chamber to avoid resuspension. The shape and position of the inflow diffusers, the conformation of the pump intake inside the chamber and the flow rate adjustment, obtained by modifying the propeller blades of the pump, were fundamental for this purpose.

Laboratory tests were carried out to verify that the chamber did not generate resuspension of sediments during the measurement due to an excessive current speed at the water-sediment interface. For this purpose, silt-clayey sediments similar to those from the 16 measurement sites were used in the test, and the absence of resuspension in the incubated water was monitored with a small camera and a turbidity sensor.

In the field, the turbidity sensor of the multi-probe used inside the benthic chamber constituted the ultimate check of the absence of resuspension phenomena throughout the measurement.

2.4 Preparation and use of the chamber in situ

Probes were calibrated prior to field campaign using specific Aquaread standards for each sensor.

The chamber was lowered by holding it by the two centimeter-steel and completely immersed in the water column. Then the pump was turned on and primed, and it was ensured that all the air was expelled from the chamber through the bleed valve; the latter was finally closed.

Hence the chamber was lowered and pushed in the bottom sediment; this step was done with care to minimize disturbance to the bottom sediment. The benthic chamber must remain completely submerged during the entire measurement period. It can be correctly deployed when the height of the water column is equal to at least 40 cm and can be used for measuring up to a minimum height of 25 cm. The final driving depth of the chamber can be precisely recorded, thanks to a centimeter scale placed on the steel rods.

The chambers were deployed for periods ranging from 100 to 200 minutes and, less frequently, beyond. Pump battery and data-logger were placed in a resealable polyethylene box, hung to a post driven into the sediment in proximity of the benthic chamber.

2.5 Blank correction

In the first period of the study, measurements were done to determine the rate of DO depletion due to the oxygen demand rate of the water incubated inside the chamber (WOD), to be subtracted (*blank correction*) from the measured DO depletion rate values (Rounds and Doyle, 1997; Doyle and Lynch, 2005). This was done by completely filling with site water a thick 10 L opaque polyethylene container, which was left at the bottom for the entire duration of the measurement. The water-column oxygen demand was then determined by comparing the DO concentration at the beginning and end of the water incubation period.

Leaving aside the following considerations, this measurement can be affected by significant errors (Caldwell and Doyle, 1995; Rounds and Doyle, 1997; Heckathorn and Gibs, 2010) as waters incubated in the measuring chamber and in the “*blank*” one may be dissimilar.

As observed in other studies (Caldwell and Doyle, 1995; Rounds and Doyle, 1997; Wood, 2001; Heckathorn and Gibs, 2010) the WOD was found to be very small (1 - 4%) compared to the measured SOD rate and its measurement was no longer deemed necessary, although it cannot be excluded that it was not negligible in particular environmental conditions encountered during the study.

2.6 SOD rate calculation

A typical plot of DO concentration depletion versus time elapsed is showed in Figure 3.

With a linear regression applied to the approximately straight section of the curve, the slope m ($\text{mg L}^{-1} \text{min}^{-1}$) was determined and the SOD was obtained as (Murphy and Hicks, 1986):

$$(1) \quad \text{SOD}_T = 1.44 * V * A^{-1} * m$$

where SOD_T is the sediment oxygen demand rate ($\text{g m}^{-2} \text{d}^{-1}$) at water temperature T ($^{\circ}\text{C}$), V is the volume of incubated water (L), A is the area of sediment enclosed by the chamber (m^2), and 1.44 is a unit-conversion factor (from mg min^{-1} to g d^{-1}).

Equation (1) can be rewritten as:

$$(2) \quad \text{SOD}_T = K * m$$

where K includes the geometric parameters of the chamber and the conversion for units of measure. Chambers used in this study were characterized by a $K = 298$; when the chamber insertion depth was slightly different from the expected 7 cm, a volume correction was made resulting in a K value in the range 270 – 327, comparable with that of other studies (Steeby et al., 2004 ($K = 260$); Ziadat and Berdanier, 2004 ($K = 363$); Doyle and Lynch, 2005 ($K = 333$); Utley et al., 2008 ($K = 347$); De Vittor et al., 2016 ($K = 305$)).

To compare SOD rates measured at different temperatures, the values are corrected to 20°C through a van't Hoff equation (Thomann and Mueller, 1987), as temperature affects the solubility of oxygen in water:

$$(3) \quad \text{SOD}_{20} = \text{SOD}_T * 1.065^{(20-T)}, T \geq 10^{\circ}\text{C} \quad (\text{no longer valid for } T < 10^{\circ}\text{C} \text{ (Rounds and Doyle, 1997)}).$$

The initial small increase of DO concentration observed in Fig. 3 is due to the water mixing inside the chamber generated by the circulation induced by the pump. The inflection of the curve that sometime occurs just below the DO concentration of 3 mg L^{-1} reflects a situation where respiration of microorganisms at the sediment surface begin to be oxygen limited. Beyond this point, this process may negatively influence the SOD rate value (Doyle and Lynch, 2005), and therefore SOD rate was calculated in the $\text{DO} \geq 3 \text{ mg L}^{-1}$ range.

Within the 9-months measuring period, some measures have not been successful, due to human errors (faucet left open, data logger not started), pump breakdown, or unavailability of a probe. A total of 141 measurements were performed at the 16 sites and the SOD rate was determined with linear regressions in the range of the coefficient of determination $R^2 > 0.94$.

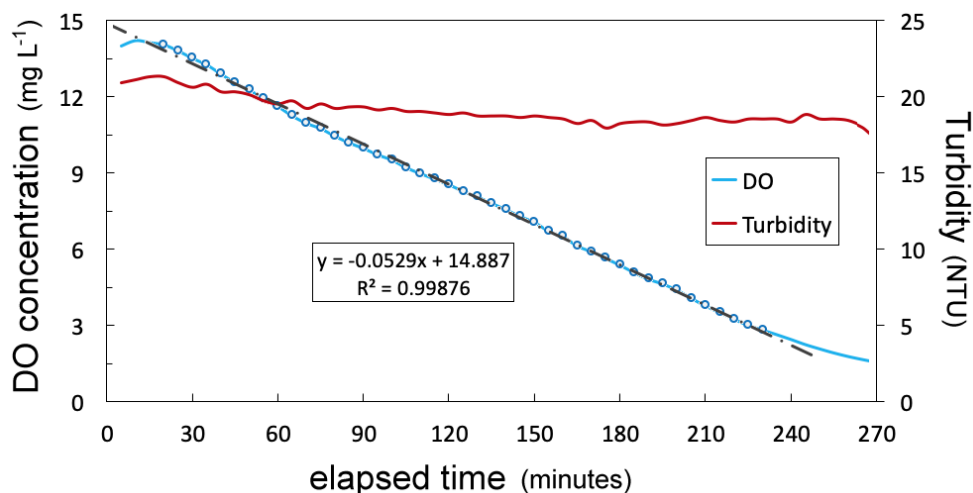


Figure 3. Example of oxygen depletion curve for a chamber placed at site CA2. The turbidity trend is superimposed. Slope m is calculated for the approximately straight section of the oxygen-depletion curve, which is highlighted with light blue dots.

2.7 Replicates

At the beginning of the study, two tests were conducted in field to verify the repeatability of the SOD rate measurement. For this purpose, 4 benthic chambers were used in a small neighborhood of a site. The obtained DO concentration depletion curves are shown in Figure 4. Low coefficients of variation (CV%) were obtained for the SOD rate (6.2 and 14.8%, respectively), which we attribute more to the heterogeneous nature of the bottom sediments than possible artifacts in the measurement.

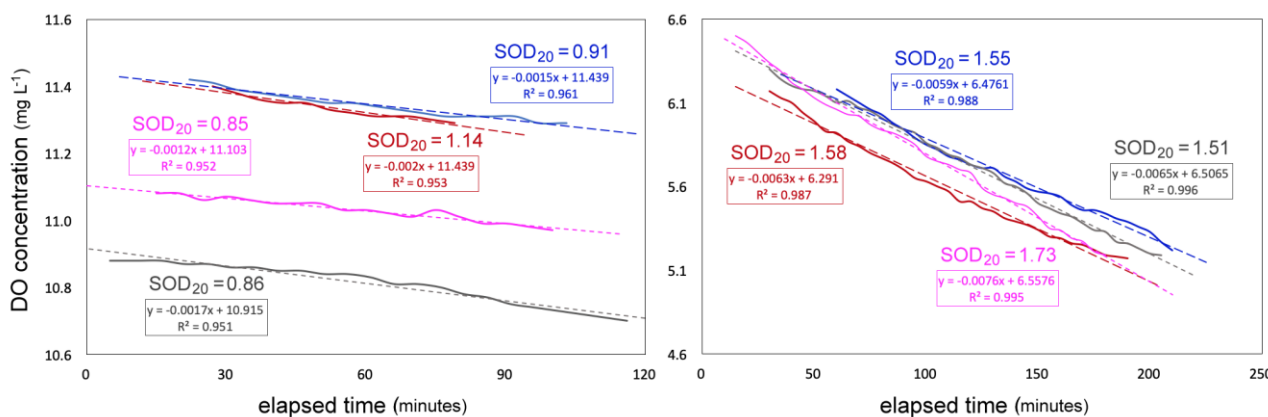


Figure 4. Results of two tests of repeatability of the SOD₂₀ rate (g m⁻² d⁻¹) measurement using 4 benthic chambers in a small neighborhood of a site.



Repeatability test of the SOD rate measurement, with 4 benthic chambers placed in a small neighborhood.

3. RESULTS AND DISCUSSION

3.1 Sediment characteristics

The sediment of the Venice Lagoon has been extensively investigated since the 1980s, in terms of composition, texture and contamination, at the scale of the entire waterbody as well as in sectors of specific interest for particular environmental problems (e.g. Zonta et al., 2018 and references therein).

Sediment analyses (TN, TOC, grain size, TIC, porosity) performed on samples from the 16 sites showed comparable values in the two sampling layers (0-1 and 1-2 cm) except for some variables in few sites, therefore the mean values between the two layers was considered (0-2 cm).

The distribution of values among sites is shown in Figure 5. Grain-size characteristics are expressed with the D50 value (median particle size), which is the corresponding particle size when the cumulative percentage reaches 50%. Data normality for each variable was verified using the Kolmogorov-Smirnov test ($p > 0.01$). Sand content in the range 63 – 500 μm is also shown.

As expected, a clear difference was observed between sites of the SS area (named Type O - *open lagoon*) compared to the others, on the basis of the values of all the variables shown in Figure 5. Belonging to the open lagoon, these sites are characterized by coarser grain size, larger presence of TIC and lower of TOC and TN, with respect to the other sites.

Among the other sites, the two most confined sites of CA (CA1 and CA2) and SG (SG1 and SG2) areas and the four sites of the PL area showed opposite values with respect to Type O (named Type C – *confined*). In particular, the higher presence of TN and TOC in these sediments is ascribable to their proximity of the lagoon edge, characterized by low water renewal times and the presence of the mouths of freshwater tributaries delivering nutrients and chemical compounds from drainage basin (Collavini et al., 2005).

SG1 has the finest median grain-size and the greatest presence of TN and TOC among the 16 sites, presumably due to the proximity of the mouth of the Osellino canal which transfers fresh water and fine particles from the drainage basin into the lagoon.

The remaining 4 sites (CA3, CA4, SG3, SG4) that are more distant from the lagoon-mainland interface within CA and SG areas, showed intermediate values (Type I - *intermediate*) of variables shown in Figure 5.

Porosity value distribution among the 16 sites (not shown in Fig. 5) reproduces the subdivision of the sites into three types.

It is worth noting that in the CA area there is a gradient of fine particle content increasing from the lagoon (CA4) towards the mainland (CA1), and the sediment of the two more confined sites had a higher concentration of TN and TOC than CA3 and CA4. Similarly, these differences are observed between the SG sites close to the mainland (SG1 and SG2) and the more distant (SG3 and SG4). With regard to these latest sites, small but significant differences are observed due to the greater proximity of SG3 compared to SG4 to a main channel which determines the tidal impulse propagation and therefore the water renewal in the area.

Although these variables were measured only once (May 2021), the data were used for evaluating the variability of the SOD₂₀ rate values with respect to the characteristics of the sediment in the 16 sites (see paragraph 3.2).

Grain size, porosity and TIC in these sites are not expected to change substantially in the short term, as evidenced by the scarce variations of the measured values between the upper layer (0-1) and the subsurface layer (1-2 cm), as well as considering previous studies (Sfriso et al., 2005; Zonta et al., 2018). Instead, it should be noted that TOC and TN may be subject to a greater annual variability.

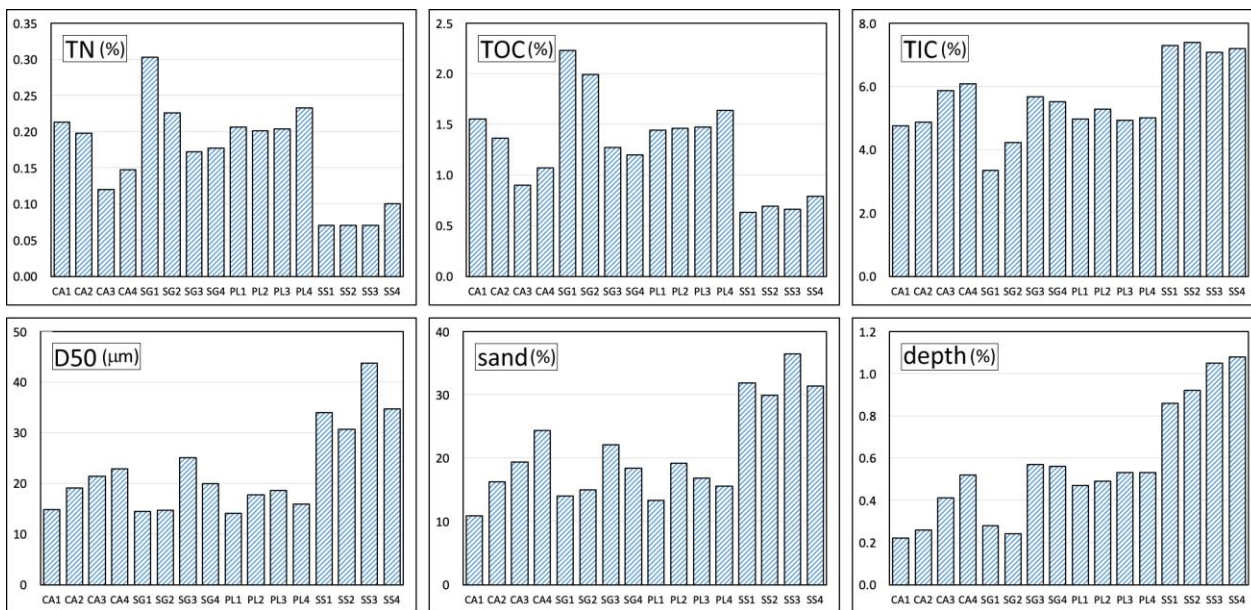


Figure 5. Total nitrogen, TOC and TIC concentration values, D50 diameter and sand content (63 – 500 µm) in the 0-2 cm sediment layer of the 16 sites, and their water depth.

3.2 SOD rate distribution with site and time

The distribution of both SOD_T and corrected SOD_{20} rate values measured in the 9-months period is shown for each site in Fig. 6, together with the water temperature measured inside the benthic chamber.

SOD_T rate values ranged from 0.63 to 24.00 $g\ m^{-2}\ d^{-1}$ and T values from 11.73 to 33.27 °C.

Higher SOD_T rate values were registered in the warm months in all sites, due to the increase with temperature of the rate of oxygen-depleting processes. A significant increase was recorded already in June in the more confined sites of CA (CA1 and CA2) and SG (SG1 and SG2) areas, whereas it occurred in July in the PL area.

A more or less significant increase in the SOD_T rate was observed at several sites towards the end of the year, despite the decrease in temperature. Particularly, in the SS3 and SS4 sites the highest values of the study were recorded in October, which remained relatively high in November. We ascribed these values to the presence of fragments of macro algae (*Ulva* and *Gracilaria*) in the water column, some of them may have become trapped in the benthic chamber, producing an extra contribution of oxygen consumption.

Correcting the SOD_T rate value by the water temperature obviously resulted in a more flattened SOD_{20} rate distribution. The latter, however, retained considerable variability between sites and months of measurement. SOD_{20} rate values ranged, in fact, from 0.87 to 14.48 $g\ m^{-2}\ d^{-1}$.

The recorded SOD_{20} rate value distributions were in agreement with the subdivision of the 16 sites in the three types, as distinguished on the basis of sediment characteristics; these, in turn, depends on the location of the site within the lagoon. Type C sites showed the highest SOD_{20} rates, whereas the lowest were recorded in the SS area (Type O). The remaining four sites (CA3, CA4, SG3, SG4), which within areas CA and SG are more distant from the lagoon-mainland interface, showed again intermediate values (Type I).

This situation is highlighted in Figure 7, where mean SOD_{20} rate values (from 1.58 to 6.16 $g\ m^{-2}\ d^{-1}$) recorded at each site over the entire measurement period are shown. Data normality for each site was verified using the Kolmogorov-Smirnov test ($p > 0.01$) after a Iglewicz and Hoaglin outlier test (Iglewicz and Hoaglin, 1993). The latter highlighted the values recorded in October in the SS3 and SS4 sites, which were excluded from the statistics.

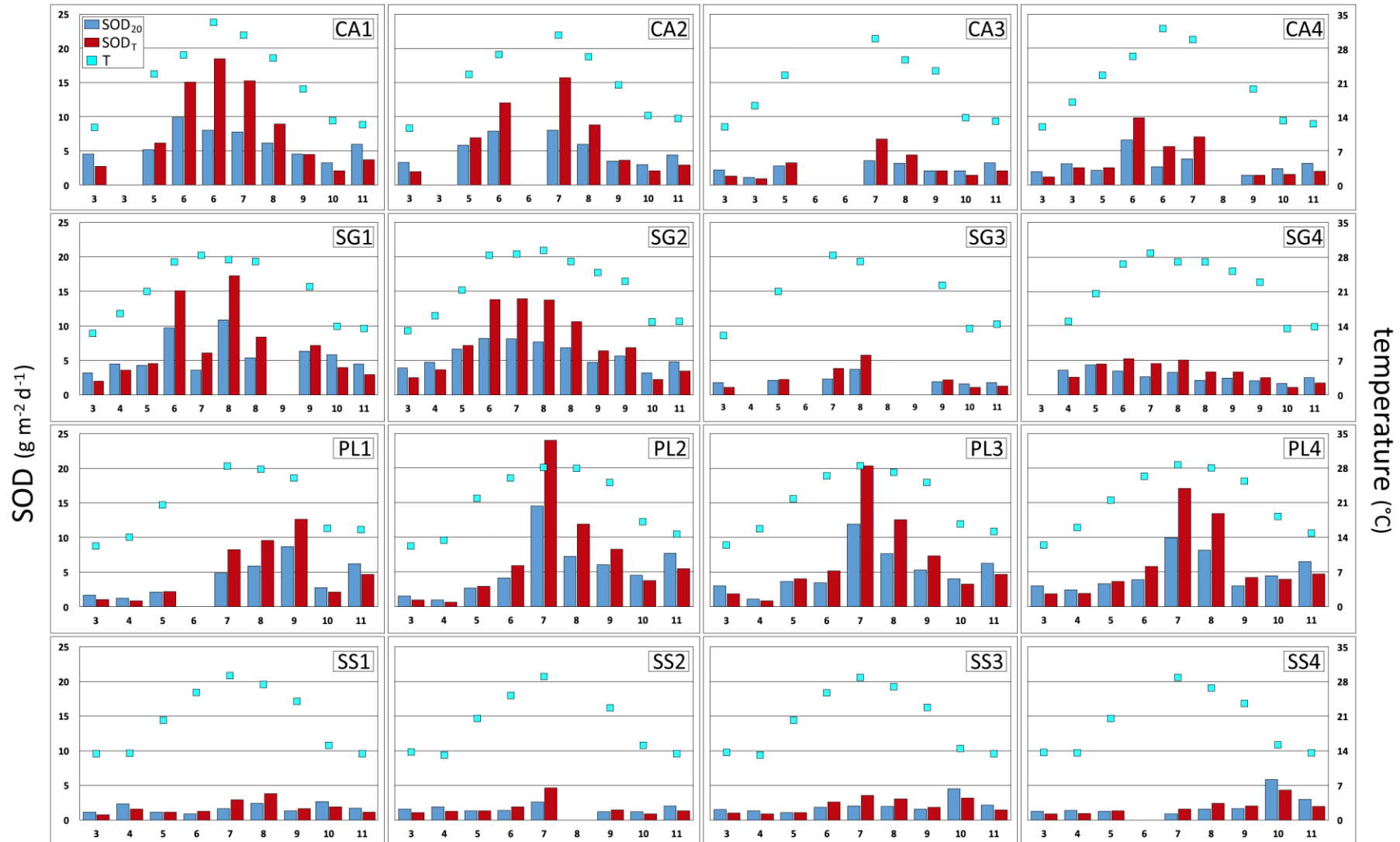


Figure 6. SOD_T and SOD₂₀ rate trend with months of 2021, in the 16 sites: water temperature measured inside the benthic chamber is also shown. Two measurements were done in the CA area in June, and two in SG both in August and September. The 14 missing measurements were due to technical problems (data logger or pump malfunction), operational errors in the deployment of the benthic chamber, or the unavailability of a probe.

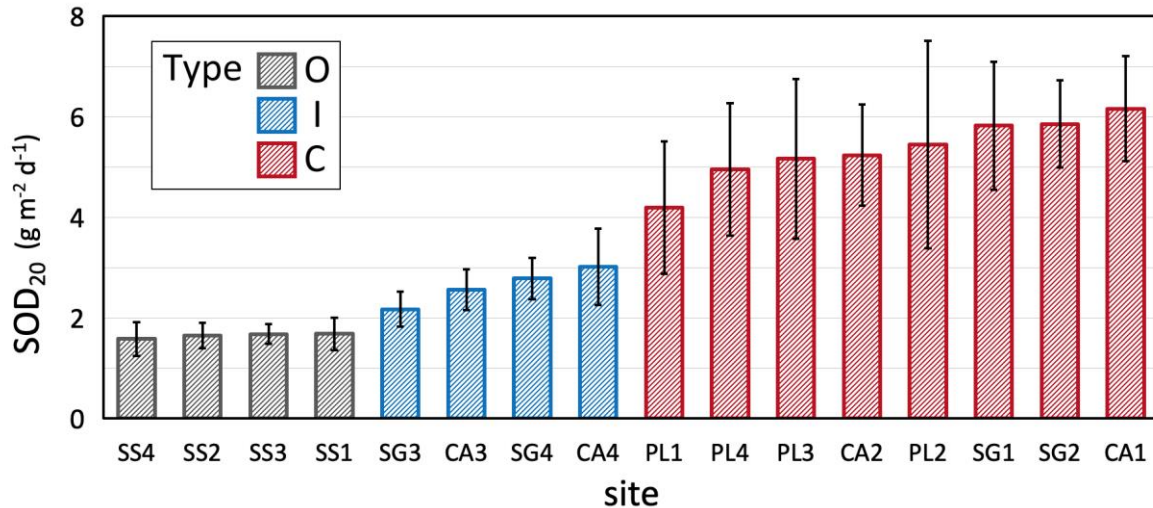


Figure 7. Mean SOD₂₀ rate for the whole period in the 16 sites, in a decreasing order; line indicates standard deviation value. Bar coloring highlights the 3 groups of sites.

Among the few studies that have concerned sediment and DO in the Venice Lagoon, Melaku Canu et al. (2003) developed an ecological model that simulated the evolution of nine ecological state variables, including DO concentration. In the mass balance components, they assumed a value of SOD₂₀ = 1.08 g m⁻² d⁻¹. On the basis of the experimental results of our study, the value assumed in the model seems excessively low, being respectively about 66 and 20% of the mean SOD₂₀ rate value measured in sites representative of the open lagoon (Type O, 1.65) and in the more confined sites (Type C, 5.35 g m⁻² d⁻¹).

The correspondence between the sediment characteristics and the average SOD rate values is clarified by the correlation matrix shown in Table 3.

Table 3. Correlation matrix calculated with the variables measured in the sediment of the 16 sites and the mean values of the SOD₂₀ rate measured in the year 2021 (the two values measured in SS3 and SS4 in October were excluded). Sand content content is in the range 63-500 μm; porosity is expressed in percentage.

	SOD ₂₀	TN	TOC	TIC	D50	sand	depth
TN	0.88						
TOC	0.88	0.97					
TIC	-0.89	-0.97	-0.96				
D50	-0.84	-0.88	-0.84	0.88			
sand	-0.85	-0.89	-0.84	0.91	0.97		
depth	-0.83	-0.81	-0.80	0.89	0.90	0.92	
porosity	0.86	0.93	0.94	-0.92	-0.85	-0.85	-0.78

Various authors have considered sediment grain size and organic matter concentration (frequently measured with the *Loss on Ignition* technique) with respect to the variation of SOD rate data in statistical analyses (e.g. Butts and Evans, 1979; Wood, 1999; Doyle & Linch, 2005; Foster et al., 2016). Generally, clear-cut relationships were not obtained but a more or less defined linear dependence.

The degree of correlation obtained in the present study was relatively elevated among all the variables involved. The reason presumably lay in both having compared mean values of SOD₂₀ measured for a long period and the selection of a set of sites with quite diversified characteristics - even if typically of the lagoon.

Two elements (regression of SOD₂₀ with respect to TN and D50, respectively) of the correlation matrix in Table 3 are shown in Figure 8, to evidence the differentiation of the 16 sites in three types. The latter is highlighted in the dendrogram of Fig. 9, obtained from a cluster analysis performed on SOD₂₀ and the three aforementioned sediment variables.

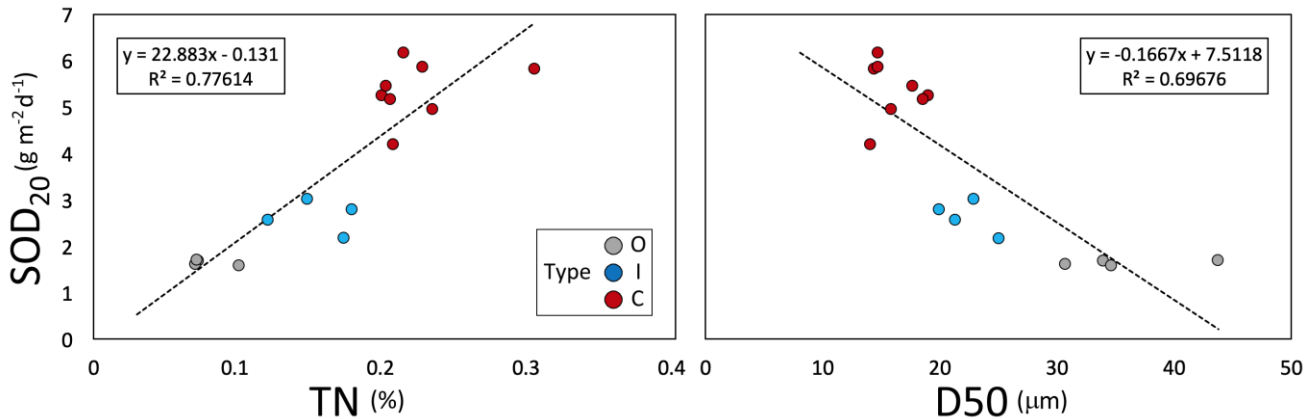


Figure 8. Regression plot between mean SOD_{20} and a) TN concentration and b) D50. The three types of sediments are evidenced with different colors.

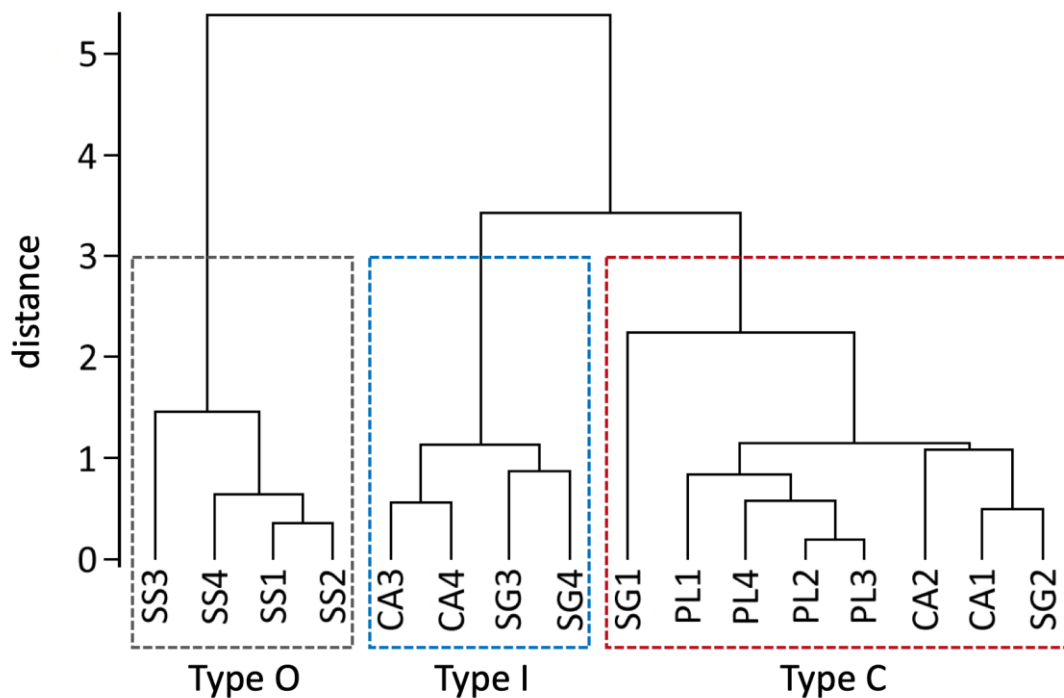


Figure 9. Dendrogram obtained from a cluster analysis performed on mean SOD_{20} rate, TN concentration and D50 data (complete-linkage hierarchical clustering).

It is important to underline how small distances in the position of a pair of sites (1 and 2) with respect to the other (3 and 4) in the SG and especially in the CA areas determined different characteristics of the sediment and consequently a different SOD rate.

The above results highlight a relation between SOD rate and sediment. In addition to the temperature, the SOD rate is influenced by variables that depend on the conditions of the water column (available oxygen, velocity of the current on the sediments, aeration), the characteristics of the sediments as well as the chemistry of the interstitial water.

The correction of SOD_T rate (equation 3) - which produces SOD_{20} rate - removes the effect of temperature on the solubility of the oxygen in the water column, but other factors still introduced a dependence of SOD_{20} on T. Observing the temporal trend of SOD_{20} (blue bars, Fig. 6), it is in fact evident the permanence of an indirect

relationship with the temperature after the rate correction, in particular in the Type C sites that in the summer period showed significantly higher values than in the other months.

Furthermore, an even more important factors are the quality and quantity of the organic matter and the composition of the biological community (Bowie et al., 1985), which changes with the availability of DO and nutrients.

The consumption of the organic matter is due to the growth dynamics of the microbial populations, which in turn are linked to temperature and organic matter supply and type, as well as the composition of the biological community and biotic interactions. Temperature affects the metabolism of oxygen-consuming microorganisms in the sediment, their density and community structure (Bowie et al., 1985; Arnosti et al., 1998; Thamdrup et al., 1998; Zakem et al., 2021).

Within physiological limits, the increase in temperature increases the rate of degradation of organic matter by microorganisms and the growth of their population, with a negative feedback process in which oxygen is the limiting factor (Zakem et al., 2021). The temperature acts both at the level of a single organism, physiologically accelerating its metabolism, and at the population level, by increasing the number of microorganisms and therefore the overall metabolism. The characteristics of the organic matter are also of considerable importance in this process, since its rate of degradation depends on its lability (Bernard and Boudreau, 1992; Kirchman et al., 2005; Fagervold et al. 2014; Zakem et al., 2021).

Labile organic matter is the first that is degraded and is therefore responsible for the “fast” oxygen consumption in the short term and supports more denitrification (Twilley et al. 1999.)

The present study was limited to acquire information on the characteristics of the sediment that may be useful in discriminating the different investigated sites and in inferring the relationship between these characteristics and the SOD rate. The dependence of the SOD rate on the presence of microbial communities and other organisms in the sediment is beyond the scope of this study.

3.3 Operation of the MOSE - Estimating DO depletion due to SOD during the closing periods.

According to the present management scenario, the MOSE barriers would temporarily isolate the Venice Lagoon from the Adriatic Sea during tides greater than 110 cm (*safe-guard threshold*, Ruol et al., 2020) above the *Punta Salute* reference level (Fig. 1). The latter is 26 cm below the current mean sea level.

The 110-cm level is a compromise between the physical protection of the city, to ensure the naval commercial traffic through the inlets to the sea, and to maintain the water exchanges between the lagoon and the sea (Trincardi et al., 2016).

When a high tide event occurs, the barriers are closed before the 110-cm level, depending on the meteorological situation (wind speed, rainfall intensity). We assume that when the MOSE closes the water level in the lagoon is equal to 90 cm, as it should happen when a normal storm surge occurs (Umgiesser, 2020).

In the absence of hydrodynamics circulation, the water will be more stagnant and the oxygen “starvation” of the sediment could have a greater negative effect on the oxygen balance. To evaluate the effect of sediment on oxygen depletion, we considered a simplified scenario: 1) the water column is stationary (no tide or wind-induced current) and sediment resuspension does not occur; 2) the water level at all sites is that corresponding to the level of 90 cm at station PS (Fig. 1); 3) the initial oxygen concentration in the water column is equal to 9.17 mg L^{-1} , i.e. the saturation concentration value at $20 \text{ }^\circ\text{C}$; 4) there is neither production nor consumption of oxygen due to aeration and processes in the water column; 5) the latter is mixed and there is not the formation of a DBL at the sediment interface.

In these conditions, the time (t_{HYP}) to reach the hypoxia value (2.8 mg L^{-1}) in the whole water column due to the SOD rate alone at the closing of the MOSE can be estimated in the 16 sites and at different temperatures.

The rate value of SOD_T was used as it reflects - unlike SOD_{20} - the effective incidence of the sediment on oxygen consumption at a given T.

In equation (2), m is expressed as the ratio between the difference in oxygen concentration at saturation and at the limit of hypoxia and the time to reach that limit, obtaining:

$$(4) \quad t_{HYP}^{BC} = (K * 6.37) * SOD_T^{-1} \quad (\text{minutes})$$

that is the time elapsing to enter in the hypoxia condition within the benthic chamber; concentration 6.37 (mg L^{-1}) is the difference between DO content in water at saturation and at the hypoxia limit.

Considering the entire water column, the time to hypoxia t_{HYP} results from a proportion:

$$(5) \quad t_{HYP} = t_{HYP}^{BC} * H * (60 * h)^{-1} = 0.57 * K * H * (10^2 * SOD_T)^{-1} \quad (\text{hours})$$

where the height of the water column at the site (H) is given by 90 cm plus the bathymetric height (Table 2), and h is the height of incubated water inside the benthic chamber; 60 is the conversion factor between minutes and hours.

Obtained values of t_{HYP} are showed in Table 4. Values range from a maximum of 368 (SS1, in March, with $T = 13.22$ °C) to a minimum of 9 hours (CA1 with $T = 33.27$ and PL2 with $T = 28.02$ °C, both in July).

Figure 10 shows the power regression obtained for the mean t_{HYP} values over selected intervals of T, for the three types of sites. Data normality for each site typology was verified using the Kolmogorov-Smirnov test ($p > 0.01$).

Type C sites were prone to reach hypoxic conditions within 48 hours of MOSE closure already at a water temperature of about 22 °C. For temperatures around 30 °C, these conditions can be reached in about half a day.

Despite being located near Type C sites, oxygen consumption in Type I sites was significantly slower and remained in the order of two days even at higher water temperatures.

Instead, no-confined Type O sites, which belong to the open lagoon, showed a greater “resistance” to the depletion of oxygen caused by the closure of the MOSE, with a t_{HYP} greater than 4 days even at the higher temperature of the water column.

Table 4. Estimated time elapsing (t_{HYP}) from the DO saturation to the limit of hypoxia values in the whole water column, due to the SOD_T rate at the MOSE closure.

date	T °C	t_{HYP} hour	T °C	t_{HYP} hour	T °C	t_{HYP} hour	T °C	t_{HYP} hour
	CA1		CA2		CA3		CA4	
16/03/21	11.74	62	11.62	90	11.84	148	11.83	184
29/03/21					16.24	215	16.90	84
17/05/21	22.66	28	22.62	25	22.45	61	22.38	86
11/06/21	26.55	11	26.72	15			26.27	22
17/06/21	33.27	9					32.00	38
20/07/21	30.65	11	30.69	11	29.96	29	29.75	31
25/08/21	25.93	19	26.24	20	25.54	44		
22/09/21	19.63	38	20.50	48	23.32	93	19.62	153
26/10/21	13.12	80	14.24	83	13.78	138	13.31	138
12/11/21	12.35	46	13.60	59	13.02	93	12.46	109
	SG1		SG2		SG3		SG4	
17/03/21	12.42	89	12.98	69	12.03	207		
16/04/21	16.43	50	15.98	47			14.81	85
17/05/21	20.96	39	21.22	24	20.91	99	20.58	49
11/06/21	26.96	12	28.27	12			26.54	42
20/07/21	28.29	29	28.53	12	28.30	57	28.72	49
03/08/21	27.36	10	29.23	12	27.02	38	27.02	44
25/08/21	26.99	21	27.02	16			26.98	67
07/09/21			24.82	27			25.15	67
22/09/21	21.91	25	23.02	25	22.20	101	22.87	89
26/10/21	13.91	45	14.64	76	13.45	207	13.36	206
12/11/21	13.38	60	14.81	50	14.30	175	13.76	130
	PL1		PL2		PL3		PL4	
24/03/21	12.26	200	12.17	233	12.42	115	12.36	118
15/04/21	14.02	237	13.33	332	15.75	251	15.95	115
14/05/21	20.58	92	21.70	71	21.84	53	21.45	59
10/06/21			25.87	35	26.41	41	26.30	37
19/07/21	28.39	25	28.02	9	28.52	11	28.59	13
23/08/21	27.78	21	27.88	18	27.15	17	28.00	16
20/09/21	25.96	16	25.00	25	25.14	29	25.27	52
25/10/21	15.83	96	17.03	56	16.74	66	18.20	54
17/11/21	15.56	44	14.58	38	15.23	46	14.72	46
	SS1		SS2		SS3		SS4	
24/03/21	13.22	368	13.69	259	13.58	298	13.60	348
15/04/21	13.42	171	13.17	223	13.21	346	13.55	328
14/05/21	20.15	237	20.49	205	20.26	278	20.45	226
10/06/21	25.70	213	25.14	146	25.68	112		
19/07/21	29.08	91	28.94	60	28.73	83	28.71	192
23/08/21	27.20	70			26.88	97	26.66	123
20/09/21	23.97	160	22.60	192	22.76	158	23.50	146
25/10/21	15.04	138	15.07	309	14.45	93	15.15	70
17/11/21	13.28	239	13.23	208	13.30	207	13.50	151

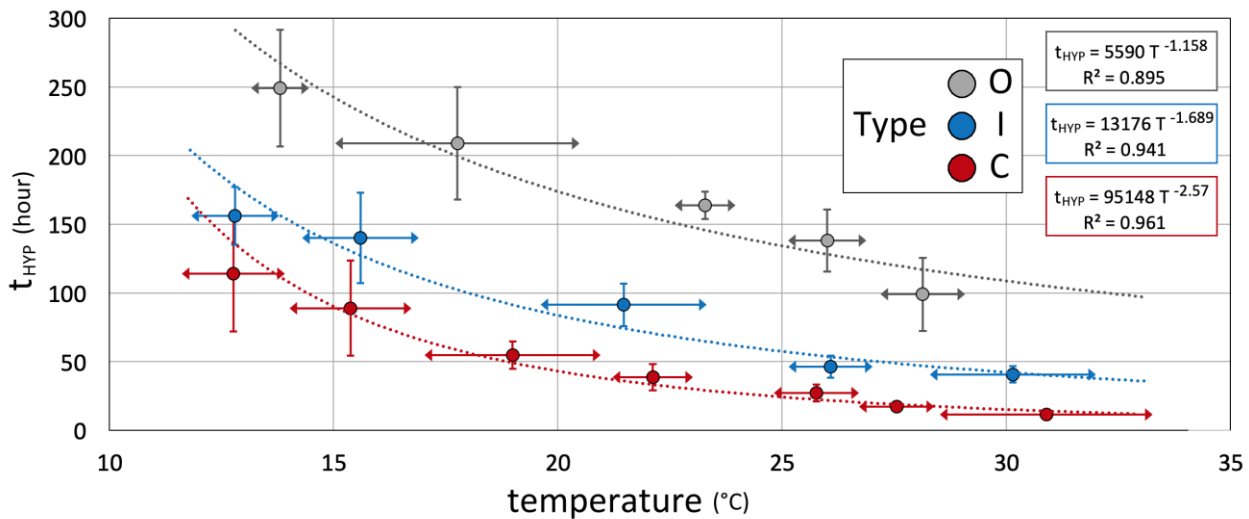


Figure 10. Plot of the relationship between temperature and t_{HYP} for the three types of sites. Dots represent mean values of t_{HYP} in selected T range, highlighted by horizontal arrows; vertical segments indicate the respective t_{HYP} standard deviation.

It is important to remember that the oxygen consumption times extrapolated in Figure 10 are calculated on the basis of the previously exposed assumptions on the water column conditions.

Nonetheless, the t_{HYP} values obtained for the different types of sites showed that in some more confined areas of the lagoon the oxygen balance can be strongly influenced by the periods of MOSE closure, even with water temperature lower than those recorded in the lagoon in the summer periods.

Brigolin et al. (2021) investigated the relation between early diagenesis in sediments and hypoxia conditions in the water column in 5 sites of the central lagoon, analyzing sediment cores at lab by means of microelectrodes. Based on the measure of the Diffusive Oxygen Uptake rates (DOU) - with an estimated error of rates at 50% - they estimated that the DO hypoxic level is reached in the water column in 5 to 18 days at $T = 25^{\circ}\text{C}$, neglecting oxygen renewal associated to primary production, exchange with the atmosphere and advection.

For open lagoon sites (Type O) our estimated t_{HYP} at 25°C is around 5 days (Fig. 10): considering that DOU makes a fraction of the Total Oxygen Uptake (TOU) (Jørgensen et al., 2022) and the factual methodological differences in the measure, the two estimates are not inconsistent.

4. CONCLUSIONS

With the aim of investigating the role of sediments on the DO balance in the water column, space and temporal variations of Sediment Oxygen Demand (SOD) rate were measured in the Venice Lagoon during the 2021. The measurements were made in situ in sixteen sites by means of benthic chambers, and produced the first dataset of SOD rate values for the lagoon. Data are useful for mathematical models aimed to the simulation of the distribution of DO concentration in the lagoon system.

A new era of “regulated flows” has begun for the lagoon as a result of the entry into operation of the MOSE system, in October 2020, which temporarily seals the water body during high tide events in the Adriatic Sea. The flow regulation is expected to lead to a general increase in the water renewal time in the lagoon, and reinforces the need to investigate the oxygen-consuming action of the sediment.

SOD rate was measured in a range of water temperature from 11.73 to 33.27 °C. The measured SOD rate values (SOD_T) ranged from 0.63 to 24.00 g m⁻² d⁻¹; once standardization was carried out at a temperature of 20 °C (SOD_{20}), the resulting range of variation was equal to 0.87 - 14.48 g m⁻² d⁻¹.

A subdivision of the sites into three typologies was observed on the basis of the distribution of SOD_{20} values and sediment characteristics. Four sites belonging to the open lagoon (named Type O - *open lagoon*), characterized by coarser particle size, greater presence of TIC and less of TOC and TN, showed lower SOD rate values. The eight more confined sites (Type C - *confined*), where sediments has opposite characteristics with respect the above type, showed instead the higher values of SOD, particularly in the hot months. The remaining four sites (Type I - *intermediate*) had intermediate both sediment features and SOD rate values.

Sediment characteristics and SOD value distribution in turn reflect different lagoon conditions, in terms of bathymetry, hydrodynamics and water renewal .

In a simplified scenario, which involved the absence of both primary production and water renewal/aeration, the incidence of sediment on the DO concentration in the water column has been evaluated at the closing of the MOSE, for the different types of sites and water temperatures. The comparison was made on the basis of the time (t_{HYP}) that elapses from the saturation of DO (9.17) to the hypoxia values (2.8 mg L⁻¹) in a still and totally mixed water column.

The t_{HYP} was found to have a power relationship with the temperature and was obviously different for the three types of sites. In the confined sites, considering only the oxygen consumption due to the sediment, DO concentration in the water column can be depleted in about a day, already at temperatures within 25 °C.

The Venice Lagoon is a varied system, where areas with similar characteristics for hydrodynamic and particle transport conditions may present sediments with different bio-geo-chemical structure. To get a more precise picture of the role of sediment in DO consumption in the water column at the whole waterbody scale, the study should be extended to a larger number of lagoon areas.

At the same time, it would be important to investigate the dependence of the SOD rate on the presence of microbial communities in the sediment, as well as the measure of the quantity and lability of the organic matter with time, accompanying the measurements to be carried out with the benthic chambers with the collection and analysis of sediment samples.

Acknowledgements

We thank Loris Dametto and Gianfranco Magris (CNR ISMAR, Venice, Italy), Daniele Curiel and Emiliano Checchin (SELC, Venice, Italy) for the support provided in the field activities. Roberto Pini (CNR IRET, Pisa, Italy) carried out the analyzes to determine sediment grain size. Leonardo Langone and Fabio Savelli (Laboratory for the measurement of N and C contents and stable isotopes - CNR ISMAR, Bologna, Italy)

performed the elementary analyzes. Paola Focaccia (CNR ISMAR, Bologna, Italy) took care of the administrative aspects of the project.

The DO% data of station S1 (SAMANET network) was provided by the Venice Water Authority (Superintendency of Public Works, Ministry of Infrastructures). Franca Pastore (Centro Previsioni e Segnalazioni Maree, Venice Municipality) provided recordings of tide and temperature data acquired from the Punta Salute tide gauge. Caterina Dabalà (CORILA) provided assistance in retrieving data from institutional measurement stations.

Funding

The study was developed within the project “Venezia 2021 - Scientific research program for a “regulated” lagoon, funded by the Venice Water Authority (Superintendency of Public Works, Ministry of Infrastructures) and coordinated by CORILA (Consortium for coordination of research activities concerning the Venice Lagoon system).

Author Contributions

Conceptualization, S.L., D.T. and R.Z.; Methodology, D.C., S.L., G.M. and R.Z.; Validation, J.D., S.L., D.T. and R.Z.; Formal Analysis, F.A., D.C., S.L. and R.Z.; Investigation, S.L., D.C., G.M., F.A. and R.Z.; Resources, D.C. and G.M.; Data Curation, S.L. and R.Z.; Writing - Original Draft Preparation, S.L. and R.Z.; Writing – Review & Editing, J.D., S.L., D.T. and R.Z.; Visualization, S.L. and R.Z.; Supervision, R.Z.; Project Administration, R.Z.; Funding Acquisition, R.Z. All authors have read and agreed to the contents of the report, and declare no conflict of interest.

References

- Altieri, A.W. and Diaz R.J., 2019. Dead zones: oxygen depletion in coastal ecosystems. In: *World Seas: An Environmental Evaluation (2nd Edition) Volume III: Ecological Issues and Environmental Impacts*. Academic Press. doi: 10.1016/B978-0-12-805052-1.00021-8.
- Arnosti C., Jorgensen, B.B., Sagemann, J., Thamdrup, B., 1998. Temperature dependence of microbial degradation of organic matter in marine sediments: polysaccharide hydrolysis, oxygen consumption, and sulfate reduction. *Mar. Ecol. Prog. Ser.*, 165, 59-70.
- ARPAV (Regional Agency for Environmental Prevention and Protection of Veneto), 2018. www.arpa.veneto.it/temi-ambientali/acqua/file-e-allegati/documenti/acque-di-transizione/rapporti-finali-e-documenti-di-classificazione-laguna-di-venezia/Risultati_monitoraggio_ecologico_2014_2016_-_Laguna_di_Venezia.pdf (*in Italian*). Accessed on Feb 18th, 2022). ^[SEP]
- Avnimelech, Y., Ritvo, G., Meijer, L. E., Kochba, M., 2001. Water content, organic carbon and dry bulk density in flooded sediments. ^[SEP]*Aquac. Eng.* 25, 25–33. doi: 10.1016/S0144-8609(01)00068-1.
- Bernard, P., Boudreau, A., 1992. A kinetic model for microbic organic-matter decomposition in marine sediments. *FEMS Microbiology Ecology*, 11, 1, 1–14.
- Bernardi Aubry, F., Aciri, F., Scarpa, G.M. and Braga, F., 2020. Phytoplankton–macrophyte interaction in the Lagoon of Venice (Northern Adriatic Sea, Italy). *Water*, 12, 2810. doi:10.3390/w12102810.
- Bowie, G. L. et al., 1985. Rates, constants, and kinetics formulations in surface water quality modeling (second edition). United States Environmental Protection Agency, EPA/600/3-85/040. p. 455.
- Breitburg, D., et al., 2018. Declining oxygen in the global ocean and coastal waters. *Science* 359, eaam7240. doi:10.1126/science.aam7240.
- Brigolin, D., Rabouille, C., Demasy, C., Bombled, B., Monvoisin, G., Pastres, R., 2021. Early Diagenesis in Sediments of the Venice Lagoon (Italy) and Its Relationship to Hypoxia. *Front. Mar. Sci.* 7:575547. doi: 10.3389/fmars.2020.575547.
- Butts, T.A. and Evans, R.L., 1979. Sediment Oxygen Demand in a Shallow Oxbow Lake. Illinois State Water Survey, Circular 136, p.28.
- Caldwell, J.M. and Doyle, M.C., 1995. Sediment Oxygen Demand in the Lower Willamette River, Oregon, 1994. U.S. Geological Survey Water-Resources Investigations Report 95–4196, p.19.
- Caraco, N. F., Caraco, J. J., 2002. Contrasting impacts of a native and alien macrophyte on dissolved oxygen in a large river. *Ecol. Appl.* 12, 1496-1509.
- Castel, J., Caumette, P. and Herbert, R., 1996. Eutrophication gradients in coastal lagoons as exemplified by the Bassin d’Arcachon and the Etang du Prevost. *Hydrobiologia* 329, ix-xxviii. doi:10.1007/BF00034542.
- Cavaleri, L., Bajo, M., Barbariol, F., Bastianini, M., Benetazzo, A., Bertotti, L., Chiggiato, J., Ferrarin, C., Trincardi, F., Umgieser, G., 2020. The 2019 flooding of Venice and its implications for future predictions. *Oceanography* 33, 42–49. DOI:10.5670/oceanog.2020.105.
- Chau, K.W., 2002. Field measurements of SOD and sediment nutrient fluxes in a landlocked embayment in Hong Kong. *Advances in Environmental Research* 6 (2), 135–142. doi: doi.org/10.1016/S1093-0191(00)00075-7.
- Collavini, F., Bettiol, C., Zaggia, L., Zonta, R., 2005. Pollutant loads from the drainage basin to the Venice Lagoon (Italy). *Environ. Int.*, 31, 7, 939-947. doi: 10.1016/j.envint.2005.05.003.
- Coenen, E.N., Christensen, V.G., Bartsch, L.A., Kreiling, R.M., and Richardson, W.N., 2019. Sediment oxygen demand: a review of in situ methods. *Journal of Environmental Quality* 48, 403-411. doi:10.2134/jeq2018.06.0251. ^[SEP]

- Collins, M., R. Knutti, J. Arblaster, J.-L. Dufresne, T. Fichet, P. Friedlingstein, X. Gao, W.J. Gutowski, T. Johns, G. Krinner, M. Shongwe, C. Tebaldi, A.J. Weaver and M. Wehner, 2013: Long-term Climate Change: Projections, Com-mitments and Irreversibility. In: Climate Change 2013: The Physical Science Basis. Contribution of Working Group I to the Fifth Assessment Report of the Intergovernmental Panel on Climate Change [Stocker, T.F., D. Qin, G.-K. Plattner, M. Tignor, S.K. Allen, J. Boschung, A. Nauels, Y. Xia, V. Bex and P.M. Midgley (eds.)]. Cambridge University Press, Cambridge, United Kingdom and New York, NY, USA, 1029-1136.
- Cucco, A., Umgiesser, G., 2006. Modeling the Venice Lagoon residence time. *Ecological Modelling* 193, 34–51. doi: 10.1016/j.ecolmodel.2005.07.043.
- De Vittor, C., Relitti, F., Kralj, M., Covelli, S., Emili, A., 2016. Oxygen, carbon, and nutrient exchanges at the sediment–water interface in the Mar Piccolo of Taranto (Ionian Sea, southern Italy). *Environ Sci Pollut Res* 23, 12566–12581. doi: 10.1007/s11356-015-4999-0.
- Diaz, R. J., and Rosenberg, R., 1995. Marine benthic hypoxia: a review of its ecological effects and the behavioural responses of benthic macrofauna. *Oceanography and Marine Biology: an Annual Review* 33, 245-303.
- Doyle, M.C., and Rounds, S., 2003. The Effect of Chamber Mixing Velocity on Bias in Measurement of Sediment Oxygen Demand Rates in the Tualatin River Basin, Oregon. U.S. Geological Survey: Water-Resources Investigations Report 03- 4097, p 17.
- Doyle, M.C., and Lynch, D.D., 2005. Sediment oxygen demand in Lake Ewauna and the Klamath River, Oregon, June 2003: U.S. Geological Survey Scientific Investigations Report 2005-5228, p.14.
- Fagervold, S.K., Bourgeois, S., Pruski, A M., Charles, F., Kerhervé, P., Vétion, G., Galand, P.E., 2014, River organic matter shapes microbial communities in the sediment of the Rhône prodelta. *ISME J.* 8, 2327–2338. doi.org/10.1038/ismej.2014.86
- Ferrarin, C., Ghezzi, M., Umgiesser, G., Tagliapietra, D., Camatti, E., Zaggia, L., Sarretta, A., 2013. Assessing hydrological effects of human interventions on coastal systems: numerical applications to the Venice Lagoon. *Hydrol. Earth Syst. Sci.* 17, 1733-1748. doi: 10.5194/hess-17-1733-2013.
- Foster, G.M., King, L.R. and Graham, J.L., 2016. Sediment Oxygen Demand in Eastern Kansas Streams, 2014 and 2015. U.S. Geological Survey Investigations Report 2016–5113, p.19.
- Garcia, H. E., and Gordon, L. I., 1992. Oxygen solubility in seawater: Better fitting equations. *Limnology and Oceanography* 37, 6, 1307–1312. <https://doi.org/10.4319/lo.1992.37.6.1307>.
- Giordani, G., Austoni, M., Zaldivar, J.M., Swaney, D.P., Viaroli, P., 2008. Modelling ecosystem functions and properties at different time and spatial scales in shallow coastal lagoons: An application of the LOTICZ biogeochemical model. *Estuarine, Coastal and Shelf Science* 77, 264-277. doi: 10.1016/j.ecss.2007.09.017
- Glud R. N., Gundersen J. K., Jorgensen B. B., Revsbech N. P., Schulz H. D., 1994. Diffusive and total oxygen-uptake of deep-sea sediments in the eastern South-Atlantic-Ocean: in situ and laboratory measurements. *Deep-Sea Research part I*, 41, 11-12, 1767-1788.
- Glud, R., N., 2008. Oxygen dynamics of marine sediments. *Marine Biology Research* 4, 243-289. doi: 10.1080/17451000801888726.
- Guerzoni, S. and Tagliapietra, D., 2006. Atlante della laguna - Venezia tra terra e mare. Marsilio Ed., Venezia (Italy), 42-43. ISBN 88-317-8764-0 (*in Italian*). English version available at the website: atlante.silvenezia.it/en/start_atlante_ns.phtml, accessed on March 8th, 2022.
- Hatcher, K.J., 1986. Introduction to part 1: Sediment oxygen demand processes. In: Hatcher, K.J. (Ed.), *Sediment oxygen demand: Processes, modeling and measurement*. Institute of Natural Resources, University of Georgia, Athens, GA, USA, 3–8.

Heckathorn, H.A. and Gibs, J., 2010. Sediment Oxygen Demand in the Saddle River and Salem River Watersheds, New Jersey, July–August 2008. U.S. Geological Survey Scientific Investigations Report 2010–5093. P.11.

Hobbs, C., H., 1983. A method for determining the dry bulk density of subaqueous sediments. *J. Sediment. Res.* 53, 663–665.

Iglewicz, B. and Hoaglin, D.C., 1993. How to detect and handle outliers. American Society for Quality Control (ASQC), Basic reference in quality control, vol. 16, p.87. ISBN 0-87389-247-X.

ISPRA and ARPAV, 2016. Monitoraggio della Laguna di Venezia ai sensi della Direttiva 2000/60/CE finalizzato alla definizione dello stato ecologico. Valutazione dei dati acquisiti nel monitoraggio ecologico 2013-2015 ai fini della classificazione ecologica dei corpi idrici lagunari. p. 114 (in Italian).

ISPRA and ARPAV, 2018. Monitoraggio della Laguna di Venezia ai sensi della Direttiva 2000/60/CE finalizzato alla definizione dello stato ecologico. Valutazione dei dati acquisiti nel monitoraggio ecologico 2014-2016 ai fini della classificazione ecologica dei corpi idrici lagunari. p. 117 (in Italian).

ISPRA and ARPAV, 2021. Monitoraggio della Laguna di Venezia ai sensi della Direttiva 2000/60/CE finalizzato alla definizione dello stato ecologico. Valutazione dei dati acquisiti nel monitoraggio ecologico 2017-2019 ai fini della classificazione ecologica dei corpi idrici lagunari. p. 112 (in Italian).

Jørgensen, B.B. and Revsbech, N.P., 1985. Diffusive boundary layers and the oxygen uptake of sediments and detritus. *Limnol. Oceanogr.* 30, 1, 111-122.

Jørgensen, B.B. and Des Marais, D.J., 1990. The diffusive boundary layer of sediments: oxygen microgradients over a microbial mat. *Limnol. Oceanogr.*, 35, 6, 1343-1355. doi: 10.4319/lo.1990.35.6.1343

Jørgensen, B.B., Wenzhöfer, F., Egger, M., Glud, R.N., 2022. Sediment oxygen consumption: role in the global marine carbon cycle. *Earth-Science Reviews* 228, 103987. doi.org/10.1016/j.earscirev.2022.103987

Kemp, W.M., Boynton, W.R., Adolf, J.E., Boesch, D.F., Boicourt, W.C., Brush, G., Cornwell, J.C., Fisher, T.R., Glibert, P.M., Hagy, J.D., Harding, L.W., Houde, E.D., Kimmel, D.G., Miller, W.D., Newell, R.I.E., Roman, M.R., Smith, E.M., Stevenson, J.C., 2005. Eutrophication of Chesapeake Bay: historical trends and ecological interactions. *Mar. Ecol. Prog. Ser.* 303, 1-29. doi: 10.3354/meps303001.

Kirchman, D.L., Malmstrom, R. R., Cottrell, M.T., 2005, Control of bacterial growth by temperature and organic matter in the Western Arctic. *Deep Sea Research Part II: Topical Studies in Oceanography*, Volume 52, Issues 24–26, 3386-3395. doi: 10.1016/j.dsr2.2005.09.005

Lionello, P., 2012. The climate of the Venetian and North Adriatic region: Variability, trends and future change. *Physics and Chemistry of the Earth* 40-41, 1-8.

MacPherson T.A., Cahoon, L.B., Mallin, M.A., 2007. Water column oxygen demand and sediment oxygen flux: patterns of oxygen depletion in tidal creeks. *Hydrobiologia* 586, 1, 235-248. doi: 10.1007/s10750-007-0643-4.

Manabe, S., Stouffer, R. J., Spelman, M. J., & Bryan, K., 1991. Transient responses of a coupled ocean-atmosphere model to gradual changes of atmospheric CO₂. Part I. Annual mean response. *Journal of Climate* 4, 8, 785–818. [https://doi.org/10.1175/1520-0442\(1991\)004<0785:TROACO>2.0.CO;2](https://doi.org/10.1175/1520-0442(1991)004<0785:TROACO>2.0.CO;2)

Mel, R.A., Viero, D.P., Carniello, L., Defina, A., D’Alpaos, L., 2021. The first operations of MOSE. system to prevent the flooding of Venice: Insights on the hydrodynamics of a regulated lagoon. *Estuarine, Coastal and Shelf Science* 261, 107547. doi: 10.1016/j.ecss.2021.107547.

Melaku Canu, D., Solidoro, C., Umgiesser, G., 2003. Modelling the responses of the Lagoon of Venice ecosystem to variations in physical forcings. *Ecological Modelling* 170, 265–289. doi: 10.1016/j.ecolmodel.2003.07.004.

- Middelburg, J. J., C. M. Duarte & J.-P. Gattuso, 2005. Respiration in coastal benthic communities. In Del Giorgio, P. A. & P. J. LeB. Williams (eds), *Respiration in Aquatic Ecosystems*, Oxford University Press, New York, 206–224.
- Molina, M.O., Sánchez, E., Gutiérrez, C., 2020. Future heat waves over the Mediterranean from an Euro-CORDEX regional climate model ensemble. *Nature* 10:8801. doi: 10.1038/s41598-020-65663-0.
- Murphy, P. J., and Hicks D. B., 1986. In situ method for measuring sediment oxygen demand. In *Sediment Oxygen Demand: Processes, Modeling and Measurement* (Edited by Hatcher K. J.), Institute of Natural Resources, University of Georgia, Athens, pp. 307-330.
- NRC, National Research Council, 2000. *Clean Coastal Waters. Understanding and Reducing the Effects of Nutrient Pollution*. National Academy Press, Washington, D.C., 393 pp.
- Percival, J.B., Lindsay, P.J., 1997. Measurement of physical properties of sediments. In *Manual of Physico-Chemical Analysis of Aquatic Sediments*; Mudrock, A., Azcue, J.M., Mudrock, P., Eds.; CRC Press: Boca Raton, FL, USA, 7–45.
- Pitcher, G.C., et al., 2021. System controls of coastal and open ocean oxygen depletion. *Progress in Oceanography* 197, 102613. doi: 10.1016/j.pocean.2021.102613.
- Rong, N., Shan, B., and Wang., C., 2016. Determination of sediment oxygen demand in the Ziya River watershed, China: Based on laboratory core incubation and microelectrode measurements. *Int. J. Environ. Res. Public Health* 13, 2, 232. doi:10.3390/ijerph13020232.
- Rounds, S., and Doyle, M., 1997. *Sediment Oxygen Demand in the Tualatin River Basin, Oregon, 1992-96*: U.S. Geological Survey on Water-Resources Investigations Report 97-4103, p.19.
- Ruol, P., Favaretto, C., Volpato, M., Martinelli, L., 2020. Flooding of Piazza San Marco (Venice): Physical Model Tests to Evaluate the Overtopping Discharge. *Water*, 12, 427. doi :10.3390/w12020427.
- Scotti, A., 2005. Engineering interventions in Venice and in the Venice lagoon. In: Fletcher, C.A., Spencer, T. (Eds.), *Flooding and Environmental Challenges for Venice and its Lagoon: State of Knowledge*. Cambridge University Press, UK, 245-256. ISBN-13 978-0-521-84046-0.
- Sfriso, A., Marcomini, A., Pavoni, B., 1987. Relationships Between Macroalgal Biomass and Nutrient Concentrations in a Hypertrophic Area of the Venice Lagoon. *Marine Environmental Research* 22, 297-312.
- Sfriso, A., Marcomini, A., Zanette, M., 1995. Heavy metals in sediments, SPM and phytozoobenthos of the Lagoon of Venice. *Marine Pollution Bulletin* 30, 2, 116-124. 10.1016/0025-326X(94)00109-M
- Sfriso, A., and Marcomini, A., 1996. Decline of *Ulva* growth in the lagoon of Venice. *Bioresource Technol.* 58, 299–307.
- Sfriso, A., Favaretto, M., Ceoldo, S., Facca, C., Marcomini, A., 2005. Organic carbon changes in the surface sediments of the Venice lagoon. *Environment International* 31, 1002 – 1010. doi: 10.1016/j.envint.2005.05.010
- Steeby, J.A., Hargreaves, J.A. Tucker, C.S., Cathcart, T.P., 2004. Modeling industry-wide sediment oxygen demand and estimation of the contribution of sediment to total respiration in commercial channel catfish ponds. *Aquacultural Engineering* 31, 247–262. doi: 10.1016/j.aquaeng.2004.05.006
- Tagliapietra, D., Zanon, V., Frangipane, G., Umgiesser, G., 2011. Physiographic zoning of the Venetian Lagoon. In: *Scientific Research and Safeguarding of Venice - Volume VII - 2007-2010 results*. CORILA Publ. (Venice, Italy), 161-164. ISBN: 9788889405215 888940521X.
- Thamdrup, B., Hansen, J. W., Jørgensen, B.B., 1998. Temperature dependence of aerobic respiration in a coastal sediment. *FEMS Microbiology Ecology*, 25, 2, 189-200. doi: 10.1111/j.1574-6941.1998.tb00472.x
- Thomann, R.V., and Mueller, J.A., 1987. *Principles of surface water quality modeling and control*. New York, Harper and Rowe, p. 291–293.

- Todd M. J., Lowrance R.R., Goovaerts P., Vellidis G., Pringle C.M., 2010. Geostatistical modelling of the spatial distribution of sediment oxygen demand within a Coastal Plain blackwater watershed. *Geoderma* 159, 1-2, 53-62. doi: 10.1016/j.geoderma.2010.06.015.
- Trincardi, F., Barbanti, A., Bastianini, M., Cavaleri, L., Chiggiato, J., Papa, A., Pomaro, A., Sclavo, M., Tosi, L., Umgiesser, G., 2016. The 1966 Flooding of Venice: What Time Taught Us for the Future. *Oceanography*, 29, 4, 178-186. doi: 10.5670/oceanog.2016.87
- Twilley, R.R., Cowan, J., Miller-Way, T., Montagna, P.A., Mortazavi, B., 1999. Benthic nutrient fluxes in selected estuaries in the Gulf of Mexico. In: Bianchi, T.S., Pennock, J.R. and Twilley, R.R. (Eds), *Biogeochemistry of Gulf of Mexico Estuaries*, chapter 6. John Wiley & Sons, Inc., 163-209.
- Utley, B.C., Vellidis, G., Lowrance, R., Smith, M.C., 2008. Factors affecting sediment oxygen demand dynamics in blackwater streams of Georgia's coastal plain. *J. Am. Water Resour. Assoc.* 44, 742-753. doi:10.1111/j.1752-1688.2008.00202.x.
- Umgiesser, G., 2020. The impact of operating the mobile barriers in Venice (MOSE) under climate change. *Journal for Nature Conservation* 54, 125783. doi: 10.1016/j.jnc.2019.125783.
- Viaroli, P., Bartoli, M., Giordani, G., Naldi, M., Orfanidis, S., Zaldivar, J.M., 2008. Community shifts, alternative stable states, biogeochemical controls and feedbacks in eutrophic coastal lagoons: a brief overview. *Aquatic Conserv: Mar. Freshw. Ecosyst.* 18, 105-117. doi: 10.1002/aqc.956.
- G. Vellidis, P. Barnes, D. D. Bosch, A. M. Cathey, 2006. Mathematical simulation tools for developing dissolved oxygen TMDLS. *American Society of Agricultural and Biological Engineers* 49, 4, 1003-1022. ISSN 0001-2351.
- Walker, R.R. and Snodgrass, W.J., 1986. Model for sediment oxygen demand in lakes. *J. Env. Eng.* 112, 25-43. doi: 10.1061/(ASCE)0733-9372(1986)112:1(25)
- Wood, T.M., 2001. *Sediment Oxygen Demand in Upper Klamath and Agency Lakes, Oregon, 1999*. U.S. Geological Survey Water-Resources Investigations Report 01-4080, p.13.
- Zaggia, L., Rosso, J., Zonta, R., 2007. Sulphate reduction in the sediment of the Venice canals (Italy). *Marine Pollution Bulletin*, 10-12, 415-424. doi: 10.1016/j.marpolbul.2007.09.004.
- Zakem, E. J., Cael B.B., Levine, N.M., 2021. A unified theory for organic matter accumulation. *PNAS* 118 (6): e2016896118 (2021) doi:10.1073/pnas.2016896118
- Ziadat, A.H. and Berdanier, B.W., 2004. Stream depth significance during in-situ sediment oxygen demand measurements in shallow streams. *JAWRA Journal of the American Water Resources Association* 40, 3, 631-638.
- Zirino, A., Elwany, H., Facca, C., Maicù, F., Neira, C., Mendoza, G., 2016. Nitrogen to phosphorus ratio in the Venice (Italy) Lagoon (2001-2010) and its relation to macroalgae. *Marine Chemistry* 180, 33-41. doi: 10.1016/j.marchem.2016.01.002.
- Zonta, R., Costa, F., Collavini, F., Zaggia, L., 2005. Objectives and structure of the DRAIN project: an extensive study of the delivery from the drainage basin of the Venice Lagoon (Italy). *Environ. Int.* 31, 7, 923-928. doi: 10.1016/j.envint.2005.05.002.
- Zonta, R., Botter, M., Cassin, D., Bellucci, L.G., Pini, R., Dominik, J., 2018. Sediment texture and metal contamination in the Venice Lagoon (Italy): A snapshot before the installation of the MOSE system. *Estuarine, Coastal and Shelf Science* 205, 131-151. doi:10.1016/j.ecss.2018.03.007.
- Zonta, R., Fontolan, G., Cassin, D. and Dominik, J., 2021. X-ray computed tomography as a tool for screening sediment cores: an application to the lagoons of the Po River Delta (Italy). *J. Mar. Sci. Eng* 9, 323. doi: 10.3390/jmse9030323.